Available online at www.sciencedirect.com

ScienceDirect

Ceramics International 35 (2009) 1063–1069

CERAMICS INTERNATIONAL

www.elsevier.com/locate/ceramint

Correlation between sintering conditions and water contact angles for Ti–O thick films screen printed on an alumina substrate

Danjela Kuščer [*], Marija Kosec, Janez Holc

Jozef Stefan Institute, Jamova 39, SI-1000 Ljubljana, Slovenia

Received 11 March 2008; received in revised form 14 April 2008; accepted 26 April 2008

Available online 16 July 2008

Abstract

TiO_2, TiO_{2-x} and Ti_3O_5 thick-film structures on corundum Al_2O_3 substrates were prepared using screen-printing technology. The screen-printed deposits were sintered up to 1500 °C in oxidising and reducing atmospheres to vary the Ti^{4+}/Ti^{3+} ratio and consequently water contact angle. The structure of the thick films was studied with an X-ray powder diffractometer (XRD). The microstructural characteristics and the chemical composition were checked with a scanning electron microscope, equipped with an energy-dispersive spectrometer (EDS). The Ti–O films, up to 55 μm thick, exhibited excellent adhesion to the substrate and had uniform grain- and pore-size distributions. Ti_3O_5 and Al_2O_3 were found to be compatible phases up to 1500 °C in a reducing atmosphere. However, rutile-type TiO_2 and Al_2O_3 are not compatible compounds at temperatures up to 1400 °C, in either oxidising or reducing atmospheres. TiO_2 and TiO_{2-x} form two types of reaction products with Al_2O_3. These reaction products were found to have various Ti/Al ratios.

Keywords: A. Films; A. Sintering; B. Interfaces; B. Microstructure-final; D. TiO_2

1. Introduction

Ever since a report about the photo-induced decomposition of water on the surface of TiO_2 in 1972 [1], semi-conductor-based photocatalysis has attracted a great deal of attention. These compounds have the ability to detoxify environmental pollutants, to decompose organic compounds, such as insecticides, pesticides and surfactants, and to purify air and water [2,3]. Some of these compounds in particular titanium dioxide, exhibit photo-induced super-hydrophilicity [4,5] in addition to photocatalysis. Photocatalysis and super-hydrophilicity mean that when using light with a specific wavelength it is possible to remove a contaminant on the TiO_2 surface, either by photo-mineralisation or by washing it away with rain [6]. When TiO_2 is irradiated with light of a specific wavelength its surface becomes more hydrophilic [7]. However, it is difficult to preserve the TiO_2 surface in this highly hydrophilic state and so efforts have been made to maintain the high hydrophilicity for longer times [8]. Recently, it was shown that the hydrophilicity of TiO_2 was improved significantly by applying a low oxygen partial pressure during the sintering of TiO_2 [9]. As a result, in the rutile TiO_2 structure the Ti^{4+} is partially replaced by Ti^{3+}, so forming TiO_{2-x} and, consequently, the contact angle of the water decreases from 67 to 26° [9].

Titanium dioxide is commonly produced in the form of films that are strongly bonded to an inert substrate such as glass or a ceramic. The most often used methods include chemical vapour deposition [10], sputtering [11,12] and chemical processes, such as the chemical solution deposition method [3,13].

The films formed using these methods are relatively thin, i.e., a few tens to a few hundreds of nanometers thick, and it was demonstrated that a 15-nm-thick titania film will adsorb only 7% of the incident UVA irradiation at 365 nm [14]. To improve the efficiency of the titania thick films, the total surface area of the coating should be increased. Two approaches are possible, i.e., increasing the specific surface area or increasing of the number of active sites by producing open porosity. It is essential, therefore, to optimise the microstructures of the films. An attempt was made to produce titania films with thicknesses from a few to a few tens of micrometers on various substrates.

---

[*] Corresponding author at: Jozef Stefan Institute, Electronic Ceramics Department, Jamova 39, SI-1000 Ljubljana, Slovenia. Tel.: +386 1477 3489; fax: +386 1477 3887.

E-mail address: danjela.kuscer@ijs.si (D. Kuščer).

0272-8842/$34.00 © 2008 Elsevier Ltd and Techna Group S.r.l. All rights reserved.

doi:10.1016/j.ceramint.2008.04.026

The typical processing method for the preparation of structures within this range of thickness is screen-printing technology [15].

The challenge with thick-film processing is to prepare a uniform, defect-free deposit with the desired chemical composition, microstructure and thickness, with good mechanical properties and adhesion to the substrate in addition to the required functional properties of the active material. During thick-film processing it is necessary to control the chemical reactivity between the active layer and the substrate at the processing temperatures as this can deteriorate the mechanical and the functional properties of the active layer [16].

The aim of the present investigation is to study the processing of Ti–O thick-film structures deposited on a corundum Al_2O_3 substrate using screen-printing technology. Our particular interest is the design of highly hydrophilic Ti–O surfaces. In our previous work we showed that the wettability of a TiO_2 ceramic can be improved by the partial reduction of Ti^{4+} by Ti^{3+} using a lower oxygen partial pressure during the sintering process [9]. For this reason the TiO_2, TiO_{2-x} and Ti_2O_3 deposits were sintered in air and in a reducing atmosphere in order to vary the Ti^{4+}/Ti^{3+} ratio in the thick-film Ti–O structures and consequently the water contact angle. The compatibility between the Ti–O-based deposits and the Al_2O_3 substrate at temperatures up to 1500 °C in air and in a reducing atmosphere has been addressed.

2. Experimental

For the experimental work, commercially available TiO_2 (99.9%) and Ti_2O_3 (99.8%) powders, both from Alfa Aesar, Karlsruhe, Germany were used.

The nonstoichiometric TiO_{2-x} powder was prepared from stoichiometric TiO_2 powder by heating it at 1400 °C in Ar/H_2 (7%). After the firing of the TiO_2 powder in a reducing atmosphere its colour dramatically changes from white to dark-brown, indicating the reduction of the Ti^{4+} to the Ti^{3+} state and the formation of nonstoichiometric TiO_{2-x}. Both TiO_2 and TiO_{2-x} crystallise in a rutile tetragonal structure at room temperature.

The Ti_2O_3, with a median particle size of 44 μm, was very coarse. Therefore, to refine the particle size, the powder was high-energy milled in a planetary mill (Retsch, Model PM 400, Hann, Germany). The milling conditions are given in Ref. [17]. Ti_2O_3 crystallises in a rhombohedral structure.

The TiO_2, TiO_{2-x} and Ti_2O_3 pastes for the screen printing were prepared from 60 wt.% of powder that was mixed with 40 wt.% of organic vehicle, comprising α-terpineol, ethylcellulose and [2-(2-butoxy-ethoxy-ethyl)] acetate. The paste was screen printed on 250-μm-thick corundum α-Al_2O_3 substrates (Coorstek, Superstrate 99.6%, denoted Al_2O_3) and pre-fired at 600 °C for 1 h to remove the organic components. The TiO_2 and TiO_{2-x} were pre-fired in air, while the Ti_2O_3 was pre-fired in vacuum in order to prevent the oxidation of Ti_2O_3 to Ti_nO_{2n-1} [9]. Samples of TiO_2 powder were then sintered at 1100, 1200, 1300 and 1400 °C for 2 h in flowing air. Samples of the nonstoichiometric TiO_{2-x} powder were fired at 1300 and 1400 °C in an Ar/H_2 (7%) atmosphere. Samples of Ti_2O_3 were sintered at 1500 °C for 2 h in Ar/H_2 (7%). All the samples were sintered with the heating rate of 5 °C/min and cooling rate of 10 °C/min.

Diffusion couples of TiO_{2-x}/Al_2O_3 and Ti_2O_3/Al_2O_3 were prepared from TiO_{2-x} and Ti_2O_3 compacts. These were then surrounded by corundum α-Al_2O_3 powder (denoted Al_2O_3) and heated at 1400 °C for 10 h in Ar/H_2 (7%).

During the thermal treatment of the samples in Ar/H_2 (7%), titanium sponges were placed ahead of and behind the sample in the furnace to trap the impurities and ensure that only uncontaminated Ar/H_2 (7%) reached the sample. The furnace tube was used exclusively for thermally treating Ti–O ceramics and so any contamination from earlier firings is ruled out. The oxygen partial pressure in Ar/H_2 (7%) was measured using a Rapido 3100 Oxygen Analyser (Cambridge Sensotec Ltd., Cambridge, UK). The amount of oxygen in the gas before entering the tube furnace was 10^{-19} ppm at room temperature and at the exit of the tube furnace where the temperature was between 400 and 500 °C it was 10^{-17} ppm. In order to check the reproducibility of the samples sintered in Ar/H_2 (7%), three samples were separately sintered at identical sintering conditions in the furnace and afterwards analysed. The results shown in Section 3 represent an average.

The X-ray powder-diffraction data were collected at room temperature on a diffractometer (Endeavor Bruker AXS, Model D4, Karlsruhe, Germany) using Cu Kα radiation. The data were collected in the 2θ range from 10 to 70°, in steps of 0.02° with an integration time of 4 s/step. The phases were identified using the PDF-2 [18] database.

A JEOL 5800 scanning electron microscope, equipped with a Tracor-Northern energy-dispersive system (EDS), was used for the overall microstructural analysis. However, prior to being analysed in the electron microscope, the samples were coated with carbon to provide electrical conductivity and to avoid any charging effects. For a standard-less analysis, the Tracor SQ standard-less analysis program, using multiple least-squares analysis and a ZAF matrix-correction procedure, was used. The samples were analysed using an accelerating voltage of 20 kV and a spectra acquisition time of 100 s. For major elements (mass fraction >0.1) an error of standard-less EDS analysis of approximately ±5% relative can be estimated.

The contact-angle measurements were performed on the as-sintered ceramic surfaces. After the sintering process the samples were removed from the furnace and put directly into a desiccator. The contact angle was measured for several samples and the reported value is an average of these measurements. A Fibro DAT 1100 Dynamic Contact Angle and Absorption Tester (Fibro Systems AB, Stockholm, Sweden) were used for the measurements. The volume of the water droplet was 4 μl.

3. Results and discussion

The microstructures of thick-film TiO_2 on an Al_2O_3 substrate are shown in Fig. 1. The TiO_2 layers sintered in air at 1100, 1200, 1300 and 1400 °C exhibit single-phase

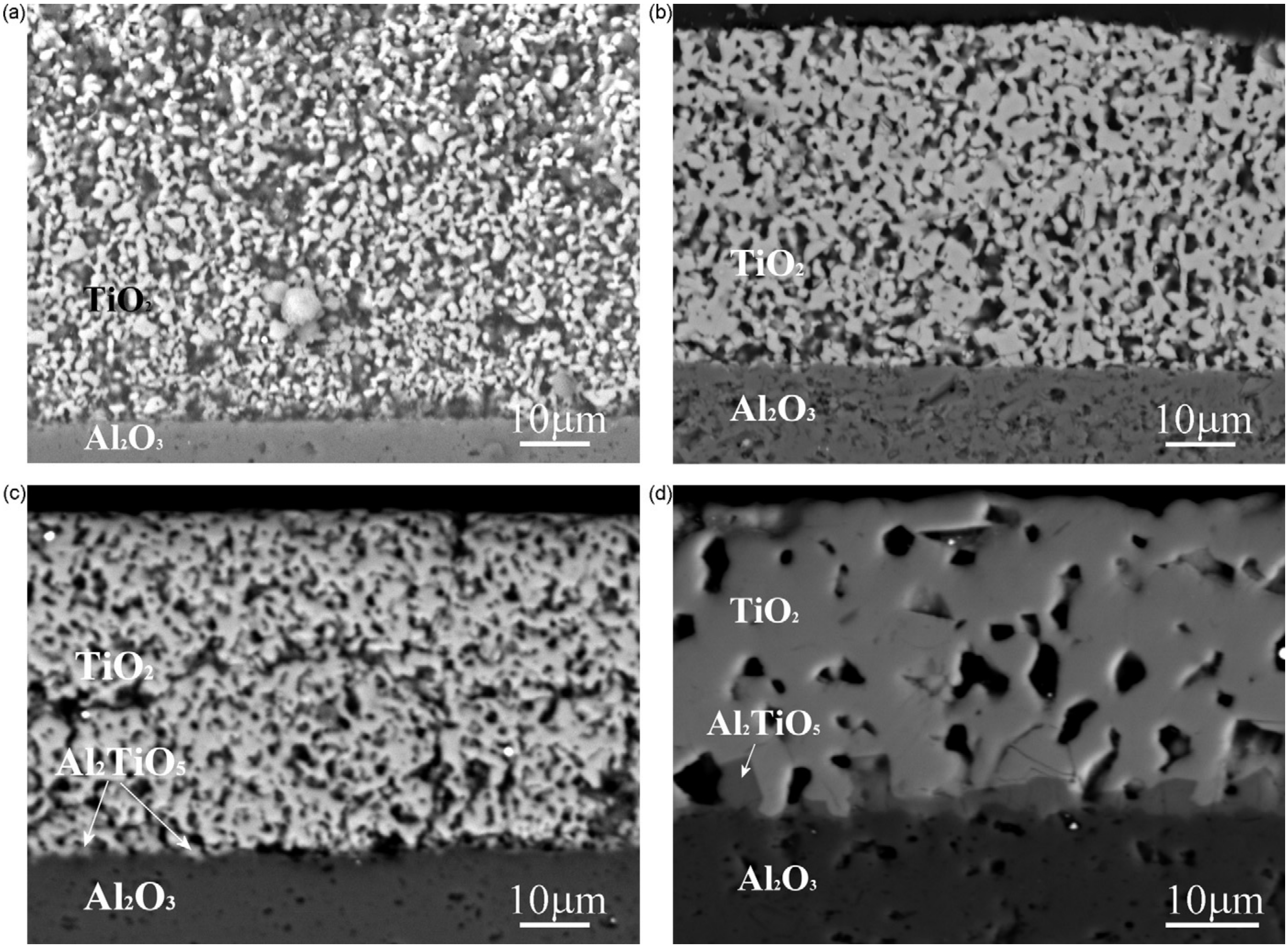

Fig. 1. Polished cross-section of screen-printed TiO_2 on Al_2O_3 substrate fired in air for 2 h at (a) 1100 °C, (b) 1200 °C, (c) 1300 °C and (d) 1400 °C.

microstructures with a homogeneous pore distribution. The thickness of the TiO_2 layer decreases with increasing sintering temperature and ranges from 55 µm at 1100 °C to 45 µm at 1200 °C and 1300 °C to 35 µm at 1400 °C.

At the TiO_2/Al_2O_3 interface no secondary phases were observed at 1100 and 1200 °C. However, the formation of a reaction product was observed in the samples sintered at 1300 and 1400 °C. A very thin reaction layer of 1 µm was observed at 1300 °C, and the thickness of this layer increased to ~5 µm when the sample was fired at 1400 °C for 2 h. This thickening of the reaction layer was expected, since the diffusion processes are promoted when we have higher temperatures and longer times. The energy-dispersive spectroscopy analysis (EDS) of the reaction product formed at 1300 and 1400 °C showed that the reaction layer consists of Al and Ti. The composition of this reaction layer was calculated using the X-ray intensities of the Al Kα = 1.48 keV and Ti Kα = 4.51 keV lines, taking into consideration the atomic number, the absorption and the fluorescence corrections. Oxygen was calculated by difference. The results show that the reaction layer contains 25 at.% Al, 12 at.% Ti and 63 at.% O, which agrees very well with the Al_2TiO_5 phase, containing, theoretically, 25 at.% Al, 12.5 at.% Ti and 62.5 at.% O. This observation is in agreement with the Al_2O_3–TiO_2 phase diagram [19], which indicates that Al_2TiO_5 is a thermodynamically stable phase in the TiO_2–Al_2O_3 system at temperatures above 1200 °C.

The microstructures of a TiO_{2-x} thick film deposited on an Al_2O_3 substrate fired at 1300 and 1400 °C in Ar/H_2 (7%) are shown in Fig. 2. The TiO_{2-x} layer is homogeneous. At the TiO_{2-x}/Al_2O_3 interface the formation of a reaction layer is observed and its thickness increases with the increasing sintering temperature. In order to determine the chemical composition of the reaction layer, the diffusion couple TiO_{2-x}/Al_2O_3 was prepared and analysed.

The SEM image and the X-ray mapping of the Al Kα and Ti Kα images of the TiO_{2-x}/Al_2O_3 diffusion couple are shown in Fig. 3. At the TiO_{2-x}/Al_2O_3 interface a 3–6-µm-thick reaction layer is observed. It is clear that the reaction layer is separated from the Ti–O ceramic by Kirkendal porosity. This phenomenon suggests that the diffusion of Ti ions into Al_2O_3 is dominant and prevails over the diffusion of Al ions into TiO_{2-x}. The EDS analysis of the reaction product shows that it contains 15 at.% Al, 20 at.% Ti and 65 at.% O. The oxygen was calculated by difference. It is evident that the composition of the reaction layer between TiO_{2-x} and Al_2O_3 is different from that between TiO_2 and Al_2O_3, which will be referred to as

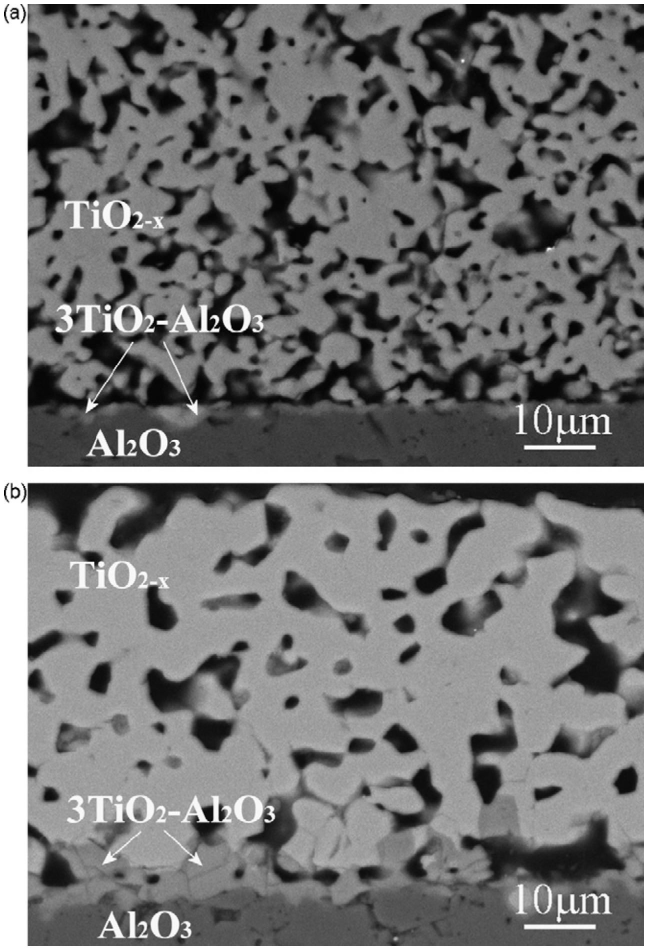

Fig. 2. Polished cross-section of screen-printed TiO_{2-x} on Al_2O_3 substrate fired in Ar/H_2 for 2 h at (a) 1300 °C and (b) 1400 °C.

$3TiO_2$–Al_2O_3. Of course, we are aware that in this case it is not possible to determine the exact composition of the reaction layer using the EDS method. However, from the results obtained it is obvious that in the reaction layers formed at the TiO_2/Al_2O_3 and TiO_{2-x}/Al_2O_3 interfaces the Ti/Al ratio is different.

TiO_2 and TiO_{2-x}, both with a rutile structure, and Al_2O_3 are not compatible phases at 1300 and 1400 °C in air or in a reducing atmosphere. TiO_2 and Al_2O_3 formed a compound, Al_2TiO_5, at temperatures above 1200 °C in air. This observation is consistent with the literature, which reports that the solubility of Ti^{4+} in Al_2O_3 is negligible but the formation of Al_2TiO_5 takes place in air at temperatures up to 1700 °C [20].

At the TiO_{2-x}/Al_2O_3 interface the formation of the reaction layer was observed, together with the Kirkendal porosity, suggesting the rapid diffusion of Ti ions into the Al_2O_3. The composition of the reaction layer formed at the TiO_{2-x}/Al_2O_3 interface is different from Al_2TiO_5 formed at the TiO_2/Al_2O_3 interface. Their compositions vary significantly in terms of the Ti/Al ratio. McKee and Aleshin [20] who studied the reactivity of TiO_2 and Al_2O_3 powders in Ar/H_2 (5%) report that when the solid solubility limit of Ti ions in Al_2O_3 is exceeded, the formation of a secondary phase is observed. The authors did not, however, determine the chemical composition of the phase, but emphasised that it is not Al_2TiO_5. Although the phase relations in TiO_2–Al_2O_3 system are well known, there is, to the best of our knowledge, no literature data on phase relations in the TiO_{2-x}–Al_2O_3 system.

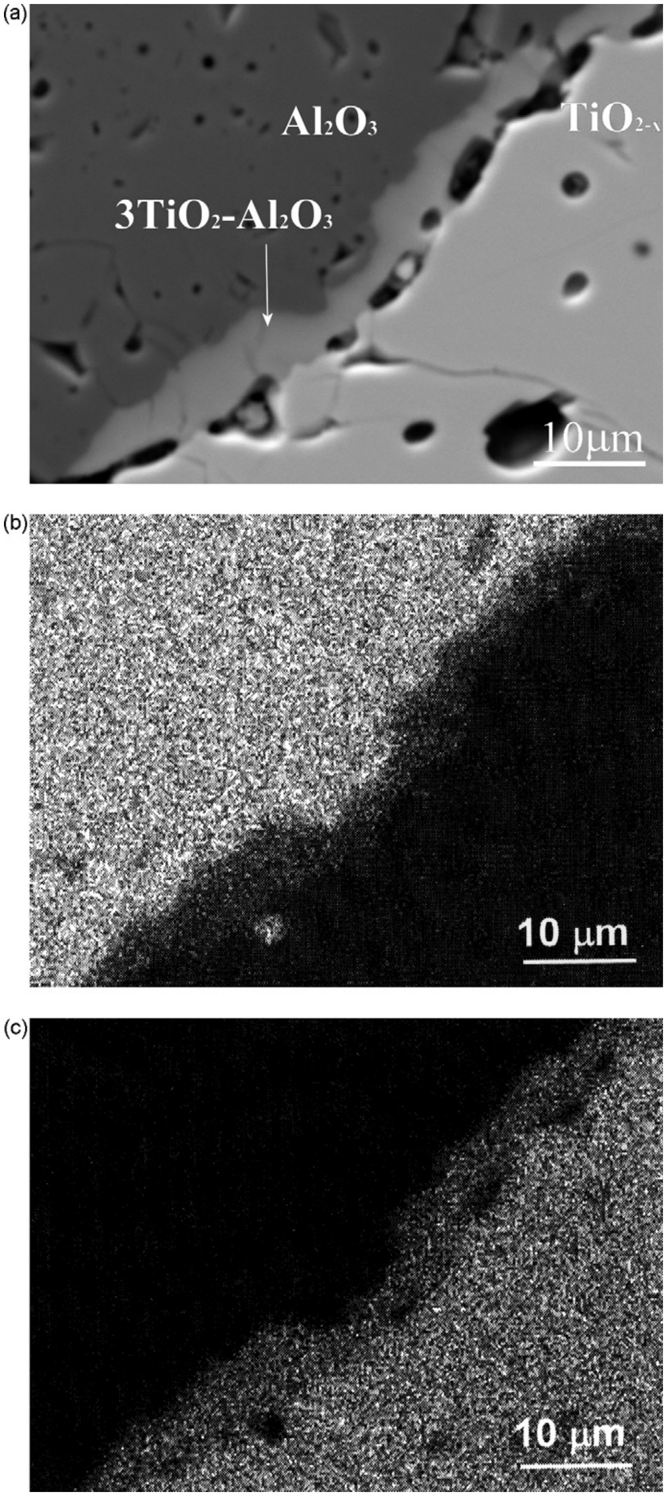

Fig. 3. Polished cross-section of nonstoichiometric TiO_{2-x}/Al_2O_3 diffusion couple aged at 1400 °C for 10 h in Ar/H_2 with X-ray maps of elements. (a) SEM/BE image, (b) Al Kα X-ray map and (c) Ti Kα X-ray map.

The microstructure of Ti_2O_3 screen-printed on an Al_2O_3 substrate and sintered at 1500 °C for 2 h in Ar/H_2 (7%) is shown

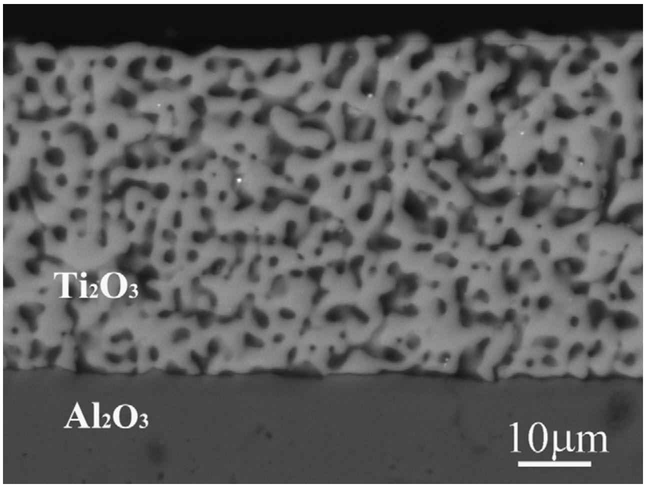

Fig. 4. Polished cross-section of Ti_2O_3 screen printed on Al_2O_3 substrate and fired at 1500 °C for 2 h in Ar/H_2.

in Fig. 4. The 40–45-μm-thick Ti_2O_3 layer is both homogeneous and porous. The screen-printed Ti_2O_3 on the Al_2O_3 exhibits a lower density than the screen-printed TiO_2 or TiO_{2-x}, even though it was sintered at a higher temperature.

The SEM image, together with the X-ray mapping of Al Kα and Ti Kα images of the Ti_2O_3/Al_2O_3 diffusion couple, is shown in Fig. 5. After annealing the Ti_2O_3/Al_2O_3 in Ar/H_2 (7%), the prevailing phase in the Ti–O system was Ti_3O_5 (PDF-ICDD 72-519) [18], with a small amount of Ti_2O_3 (PDF-ICDD 10-0063) [18] and Ti_4O_7 (PDF-ICDD 11-0219) [18], as observed using X-ray powder-diffraction analyses (Fig. 6). To the best of my knowledge, only the high temperature, gamma Ti_3O_5 phase is compatible with the corundum. For this reason the Ti–O ceramic in the Ti_2O_3/Al_2O_3 diffusion couple will be referred to as Ti_3O_5. According to Fig. 5 the diffusion of Al ions into the Ti–O accompanied by the enhanced densification of the Ti–O ceramic in this region takes place. The dense layer is 15 μm thick. From the X-ray mapping images it is evident that this region contains Ti and Al and that the amount of Al decreases from the Ti_3O_5/Al_2O_3 interface into the Ti_3O_5. The EDS analysis shows that the amount of Al_2O_3 decreases almost linearly from the Al_2O_3/Ti_3O_5 interface into the Ti_3O_5 (Fig. 7).

The obtained results show that Ti_3O_5 and Al_2O_3 are compatible phases up to 1400 °C in a reducing atmosphere. The formation of a secondary phase was not observed between Ti_3O_5 and Al_2O_3 in the screen-printed structure and in the Al_2O_3/Ti_3O_5 diffusion couple. The diffusion of Al ions into the Ti_3O_5 was observed in the diffusion couple, which improves the densification of the Ti_3O_5. To the best of our knowledge there are no data in the literature about the influence of Al_2O_3 on the sintering of Ti_3O_5 in a reducing atmosphere.

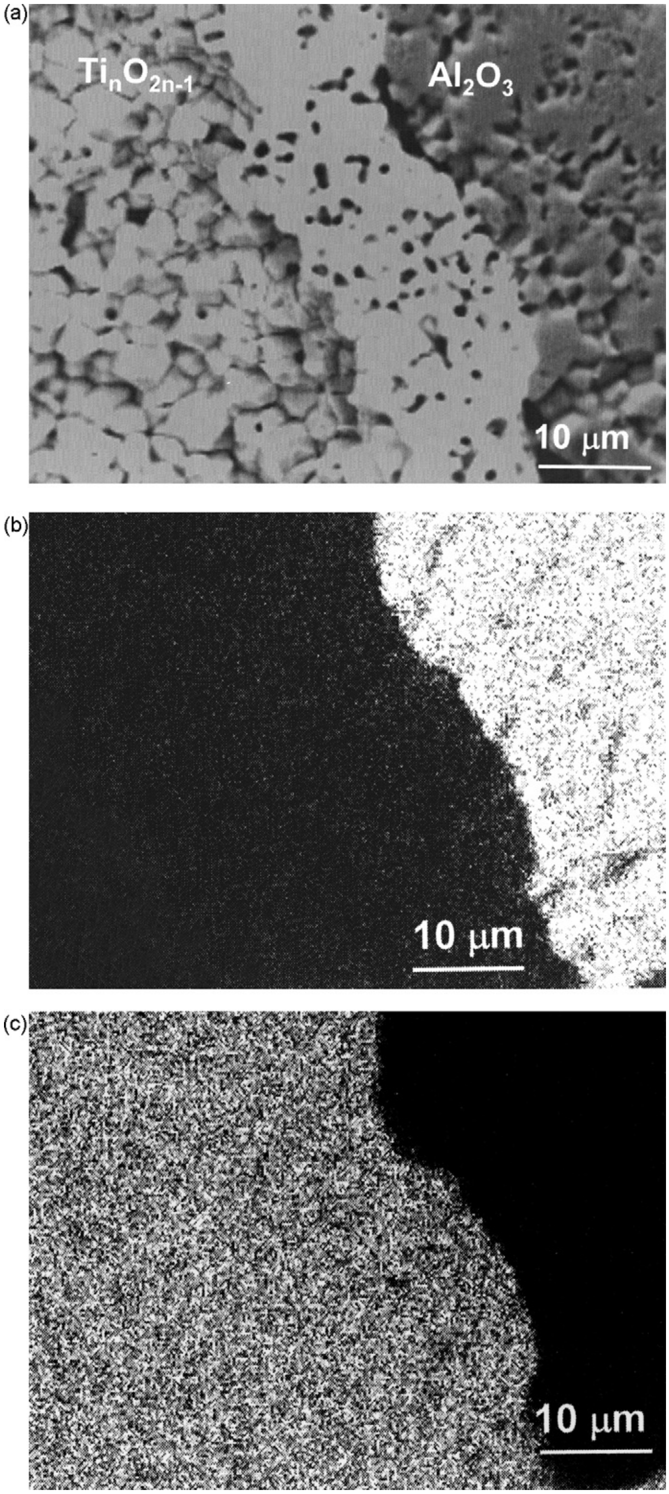

Fig. 5. Polished cross-section of Ti_2O_3/Al_2O_3 diffusion couple aged at 1400 °C for 10 h in Ar/H_2 with X-ray maps of elements. (a) SEM/BE image, (b) Al Kα X-ray map and (c) Ti Kα X-ray map.

The contact angles for water on the as-sintered thick-film surface of TiO_2 fired at 1400 °C in air, the nonstoichiometric TiO_{2-x} sintered at 1400 °C in Ar/H_2 (7%) and the Ti_3O_5 sintered at 1500 °C in Ar/H_2 (7%) are $65 \pm 2°$, $50 \pm 2°$ and $30 \pm 5°$, respectively. A water contact angle measured on the TiO_2's thick-film surface is consistent with the measurements on bulk TiO_2 [9,21]. The water contact angles measured on the TiO_{2-x} and Ti_3O_5's thick-film surfaces are lower compared to that of TiO_2. We believe that the decrease in water contact angle is a consequence of partial reduction of Ti^{4+} to Ti^{3+} during the thermal treatment of the samples in Ar/H_2 (7%). The reduction of Ti^{4+} to Ti^{3+} in titania ceramic during sintering at lower

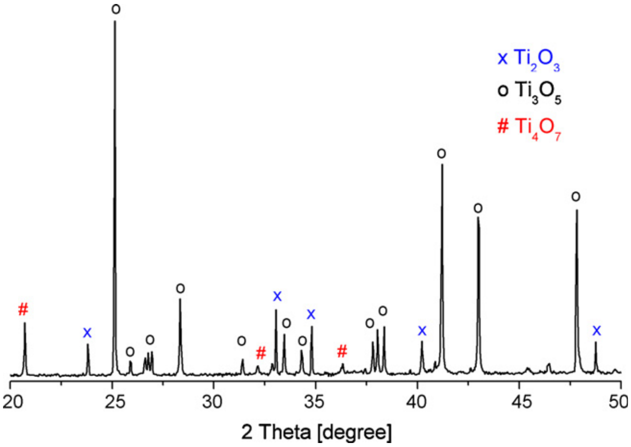

Fig. 6. XRD pattern of Ti–O ceramic from the Ti_2O_3/Al_2O_3 diffusion couple.

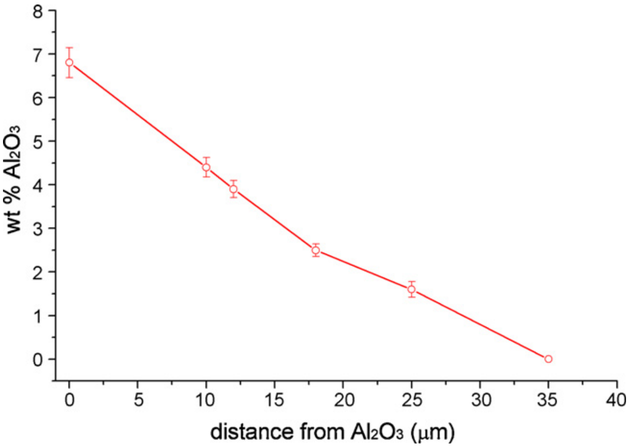

Fig. 7. The amount of Al_2O_3 in the dense region of the Ti_2O_3/Al_2O_3 diffusion couple as a function of distance from Al_2O_3.

oxygen partial pressure is well known and is already explained for bulk Ti–O in the literature [9]. The reduction is accompanied by a colour change from yellowish for TiO_2 to black for TiO_{2-x}. We have observed that the samples after the sintering in Ar/H_2 (7%) become black therefore we suppose that the reduction of Ti^{4+} to Ti^{3+} occurred during the sintering in Ar/H_2 (7%). The obtained results show that the hydrophilicity of Ti–O based thick-films can be improved significantly by decreasing the oxygen partial pressure during the sintering.

4. Summary

Thick-film structures in the Ti–O system were prepared on Al_2O_3 substrates using screen-printing technology. The procedure for fabricating Ti–O structures with various Ti^{4+}/Ti^{3+} ratios involved controlling the pre-firing step and applying oxidising and reducing atmospheres during the sintering. TiO_2, TiO_{2-x} and Ti_2O_3 pastes, prepared from micron-sized powder and an organic vehicle, were screen-printed, pre-fired in air or vacuum, followed by sintering in an oxidising or reducing atmosphere at temperatures up to 1500 °C. The sintered Ti–O structures, i.e., TiO_2, TiO_{2-x} and Ti_3O_5, have excellent adhesion to the Al_2O_3 substrate. The microstructure of the active layers is homogeneous with a uniform grain- and pore-size distributions. TiO_2 and Al_2O_3 are compatible phases up to 1200 °C in air. However, above this temperature they form the Al_2TiO_5 phase. In a reducing atmosphere TiO_{2-x} and Al_2O_3 form a phase with different Ti/Al ratios than in Al_2TiO_5 above 1300 °C. Ti_2O_3 was screen-printed on an Al_2O_3 substrate and then oxidised to Ti_3O_5 during the thick-film processing. The sintered Ti_3O_5 layer on Al_2O_3 has good adhesion to the substrate and exhibits a lower density than the TiO_2 and TiO_{2-x} thick films. At 1400 and 1500 °C the diffusion of Al ions into the Ti_3O_5 was observed, but without the appearance of any additional phase.

The hydrophilicity of Ti–O thick films can be improved by lowering oxygen partial pressures during the sintering. The water contact angle of TiO_2 on Al_2O_3 sintered in air is 65° and decreases to 50 and 30° for TiO_{2-x} and T_3O_5, respectively, both sintered in Ar/H_2 (7%).

Acknowledgments

This research was supported by the project EZPLATE No. 030 898. Mr. Silvo Drnovšek is acknowledged for the screen printing. Dr. Steven Lezy and Dr. Ronn Andriesen are acknowledged for water contact measurements and valuable discussions.

References

[1] A. Fujishima, K. Honda, Electrochemical photolysis of water at a semiconductor electrode, Nature 238 (1972) 37.
[2] A. Mills, S. LeHunte, An overview of semiconductor photocatalysis, J. Photochem. Photobiol. A: Chem. 108 (1997) 1–35.
[3] R. Fretwell, P. Douglas, An active, robust and transparent nanocrystalline anatase TiO_2 thin film—preparation, characterisation and the kinetics of photodegradation of model pollutants, J. Photochem. Photobiol. A: Chem. 143 (2001) 229–240.
[4] A. Fujishima, T.N. Rao, D.A. Tryk, Titanium dioxide photocatalysis, J. Photochem. Photobiol. C: Photochem. Rev. 1 (2000) 1–21.
[5] O. Carp, C.L. Huisman, A. Reller, Photoinduced reactivity of titania dioxide, Prog. Solid State Chem. 32 (2004) 33–177.
[6] A. Mills, G. Hill, S. Bhopal, I.P. Parkin, S.A. O'Neill, Thick titanium dioxide films for semiconductor photocatalysis, J. Photochem. Photobiol. A: Chem. 160 (2003) 185–194.
[7] N. Stevens, C.I. Priest, R. Sedev, J. Ralston, Wettability of photoresponsive titanium dioxide surfaces, Langmuir 19 (2003) 3272–3275.
[8] D. Noguchi, T. Sakai, T. Nagatomo, Photoinduced hydrophilicity and structural evaluation of SiO_x:OH/TiO_2 multilayer films by DC reactive magnetron sputtering, Jpn. J. Appl. Phys. 45 (3A) (2006) 1775–1782.
[9] D. Kuscer, J. Kovač, M. Kosec, R. Andriesen, The effect of the valence state of titanium ions on the hydrophilicity of ceramics in the titanium–oxygen system, J. Eur. Ceram. Soc. 28 (2008) 577–584.
[10] A. Mills, N. Elliott, I.P. Parkin, S.A. O'Neill, R.J. Clark, Novel TiO_2 CVD films for semiconductor photocatalysists, J. Photochem. Photobiol. A: Chem. 151 (2002) 171–179.
[11] M.C. Barnes, A.R. Gerson, S. Kumar, N.-M. Hwang, The mechanism of TiO_2 deposition by direct current magnetron reactive sputtering, Thin Solid Films 446 (2004) 29–36.
[12] S.K. Zheng, G. Xiang, T.M. Wang, F. Pan, C. Wang, W.C. Hao, Photocatalytic activity studies of TiO_2 thin films prepared by RF magnetron reactive sputtering, Vacuum 72 (2003) 79–84.
[13] M. Haraguchi, F. Komatsu, K. Tajiri, T. Okamoto, M. Fukui, S. Kato, Fabrication and optical characterization of a TiO_2 thin film on a silica microsphere, Surf. Sci. 548 (1–3) (2004) 59–66.

[14] A. Mills, S.K. Lee, A. Lepre, I.P. Parkin, S.A. O'Neill, Spectral and photocatalytic characteristics of TiO_2 CVD films on quartz, Photochem. Photobiol. Sci. 1 (2002) 865–868.

[15] J.S. Reed, Principles of Ceramic Processing, 2nd ed., John Wiley & Sons, New York/Chichester/Brisbane/Toronto/Singapore, 1995, p. 566.

[16] J. Holc, M. Hrovat, M. Kosec, Interactions between alumina and PLZT thick films, Mater. Res. Bull. 34 (1999) 2271–2278.

[17] D. Kuscer, A. Meden, J. Holc, M. Kosec, The mechano-synthesis of lead–magnesium–niobate ceramics, J. Am. Ceram. Soc. 89 (10) (2006) 3081–3088.

[18] PDF-ICDD, PCPDFWin Version 2.2, June 2001, International Centre for Diffraction Data, 2002.

[19] P. Pena, S. DeAza, The system ZrO_2–Al_2O_3–TiO_2, Ceramica 33 (3) (1980) 23–30.

[20] W.D. McKee, E. Aleshin, Aluminium oxide–titanium oxide solid solution, J. Am. Ceram. Soc. 46 (1) (1963) 54–58.

[21] R. Wang, K. Hashimoto, A. Fujishima, M. Chikuni, E. Kojima, A. Kitamura, M. Shimohigoshi, T. Watanabe, Light-induced amphilic surfaces, Nature 388 (1997) 431–432.